Neutral atom and molecule focusing using a Fresnel zone plate

Thomas Reisinger[a] and Bodil Holst
Department of Physics and Technology, University of Bergen, Allégaten 55, N-5007 Bergen, Norway

(Received 9 July 2008; accepted 25 August 2008; published 1 December 2008)

Focusing of neutral atoms and molecules has several potential applications. The very first microscopy images using helium as an imaging probe were published earlier this year. Another possible application is to study the diffusion of atoms and molecules through materials with high spatial resolution by stepping a porous or permeable sample across the focused beam. With this application in mind, the authors present the best resolution transmission images hitherto achieved with helium atoms (less than 2 μm) of a thin carbon film with 2 μm holes. Furthermore, they present the first experiment using a Fresnel zone plate to focus neutral molecules. They used a beam of deuterium (D_2) which was focused down to 15.2 ± 0.5 μm. D_2 was chosen because it fits in mass to the geometry of our system, which is optimized for helium. However, the method can be extended to hydrogen (H_2) or other molecules by using a suitably adapted zone plate. In both cases the focus was limited by chromatic aberrations, caused by the velocity spread of the beams. Finally, they present calculations exploring the resolution limits for focusing of molecular beams using Fresnel zone plates. The calculations show that Fresnel focusing down to 170 nm full width at half maximum is possible with presently available techniques. © *2008 American Vacuum Society.*
[DOI: 10.1116/1.2987955]

I. INTRODUCTION

New imaging techniques have triggered gigantic steps forward numerous times in the history of science. Past century's electron microscope[1] or scanning tunneling microscope[2] not to mention numerous advances in electromagnetic radiation imaging techniques spanning from x rays to light microscopy are just a few examples.

The topic of this article is the application of focused neutral beams in new imaging and focusing experiments. We employ supersonic free-jet expansion of atomic helium and D_2 as beam sources. Such sources are used extensively employing different molecules and atoms. For example, they are well established in techniques for the investigation of surface structure and dynamics in reciprocal space[3] and enable the measurement of interaction potentials between molecules and surfaces.[4] Other applications of molecular beams include the study of interaction potentials between molecules.[5,6]

For the focusing of such beams the primary goal is to create a microscope that uses neutral particles as an imaging probe. However, additional future focusing applications include the study of diffraction from single-crystal grains (microcrystallites) and the location-resolved study of porous or permeable membranes. In the following paragraphs we will first discuss neutral helium microscopy and then the latter application of studying membranes in the light of the D_2 beam focus also presented in this article.

The idea of utilizing a helium beam for matter-wave microscopy is not new,[7] but was demonstrated for the first time to full extend earlier this year, when the first micrograph using neutral helium atoms as an imaging probe was published[8] (see also Nature Research Highlights[9]).

The main properties setting neutral helium atom microscopy aside from existing techniques are the beam's neutrality and low energy (about 50 meV) at small wavelengths (about 0.05 nm). Electron microscopes, x-ray microscopes (also based on zone plates), as well as the new helium ion microscope[10] all operate with beam energies in the keV range or more. Furthermore the neutral helium atom microscope is the only technique which is strictly surface sensitive. There is absolutely no penetration into the material. The helium atom interacts with the outermost electron layer of the surface,[3] as opposed to the nuclei which is the case for these other high-energy methods. The neutral atoms impinging on a sample's surface do not cause charging, and therefore do not require the deposition of conductive layers. Further, the low energy entails that no sputtering occurs, in fact, the low energy is hardly enough for the beam to have an effect on adsorbed atoms. This could be exploited for example in the study of hydrogen physisorption, an effect which is considered as an option for hydrogen storage.[11]

Two main technical challenges in developing a neutral helium microscope are the designing of beam manipulating elements and high efficiency detectors. In tackling the first the problem is that the helium atoms are neutral and in their ground states and hence cannot be manipulated using electric or magnetic methods employed in electron and ion microscopy or other branches of atom optics. The most promising solution is to exploit the wave nature of atoms and molecules. As first revealed by de Broglie,[12] matter particles exhibit a wavelength given by $\lambda = h/p$, where h is Planck's constant and p the particle's momentum. An atom focus can be achieved by diffracting atoms, using Fresnel zone plates.[13,14] A zone plate is a circular diffraction grating with decreasing lattice constant for increasing radii.[15] Fresnel zone plate focusing has the advantage that the focusing ele-

[a]Electronic mail: thomas.reisinger@uib.no

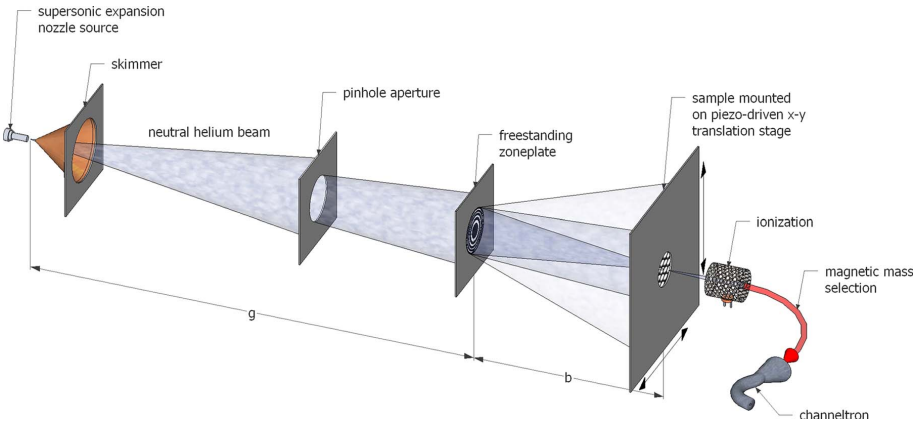

FIG. 1. Setup of the supersonic expansion beam apparatus is depicted schematically. The beam originating from a supersonic expansion is focused using a zone plate. The sample is located in the focal plane and stepped across the beam focus using a piezotable. For the D_2 focusing experiment this sample was replaced by a 5 μm slit. The transmitted particle flux is recorded using an electron bombardment detector. The source distance was $g=1492\pm5$ mm and the image distance was $b=763\pm5$ mm for helium and $b=800\pm5$ mm for D_2. For the helium micrographs the diffraction orders apart from the first were suppressed using an order selecting aperture (diameter=100 μm) located on top of the sample.

ment can be inserted directly into the beam line. It was also the technique of choice for the images presented in this article. The problem with zone plates is that they suffer from chromatic aberration and it is not possible to create a perfectly monochromatic helium beam (this will be discussed in more detail later). Another viable strategy is to diffract helium atoms off an electrostatically deformed ultraflat surface (single crystal)[7] (using the zeroth order specular peak), resulting in a minimal focus so far[16] of about 25 μm. The mirror technique's big advantage is that it does not suffer from chromatic aberration since it exploits specular scattering. However, in practice it has been proven very difficult to create the required mirror shape and to obtain a surface of high reflectivity.[16]

The second big challenge is to make a high efficiency detector. The electron bombardment detector[17] utilized in our apparatus has an efficiency of about 2×10^{-6}. However, the ongoing development of field ionization detectors using tungsten tips and carbon nanotubes gives rise to optimism.[18–21] In particular, the possibility of a two-dimensional array of carbon nanotubes used as a location sensitive detector has the potential to revolutionize the field. This will be particularly important when moving from transmission (shadow image) to exploiting the surface-only sensitivity of neutral helium atoms in a reflection microscope. For a discussion of imaging and contrast in a reflection helium microscope, see Ref. 22.

In principle the resolution in a helium microscope is limited by the wavelength of the atom (about 0.05 nm as mentioned earlier). In practice source size and various types of aberration reduce resolution.

A second interesting application of focused molecular beams, which so far has not been discussed in literature, is to use a focused beam to measure diffusion properties of materials. The idea is to step a thin porous or permeable sample across the beam focus. The molecules are detected as they emerge on the other side, having diffused through the material. This could be very interesting, for example, for the investigation of fuel cell storage materials. We envisage using a chopped beam which will enable diffusion constants and the rate of physisorption to be determined by applying time-of-flight analysis—a technique extensively employed in helium diffraction experiments. The problems of obtaining good focusing elements and high efficiency detectors are equally important for this application as for direct imaging.

To the careful reader it may perhaps seem surprising that diffractive focusing of molecules is possible to begin with. One possibility for the molecular beam's coherence to be disturbed is the excitation of rotational degrees of freedom[23] through van der Waals interaction with the Fresnel zone plate. The loss in coherence implies a degradation in focusing efficiency depending on the strength of this interaction. A simple comparison of the van der Waals field strength with the rotational energy levels of the molecule yields a reasonable approximation for how likely it is for the zone plate to induce rotational excitations. While the spacing between rotational energy levels for D_2 is of the order of tens of meV,[23] the van der Waals field is closer to being of the order of 1 μeV for a distance of 5 nm ($\frac{1}{10}$ of the smallest zone width). Here we assumed that the van der Waals coefficient for D_2 with silicon nitride[24] of $C_3=0.33$ meV nm^3 is of similar magnitude for the interaction between D_2 and nickel, which is the material the zone plate is made of. We therefore conclude that no significant effect on diffractive focusing of D_2 is to be expected. However, for large highly polarizable molecules this is likely to be an issue.

II. EXPERIMENT

The experimental setup is shown schematically in Fig. 1. A platinum Laval-type nozzle with a diameter of 10 μm is used to adiabatically expand pressurized helium (up to 200 bar) or D_2 (for this experiment 10 bar) into a vacuum chamber in a supersonic free-jet expansion. In the source vacuum chamber a pressure of about 10^{-4} mbar is sustained with a 3800 l/s (He) turbo pump. The beam-particle trajectories appear to originate from a transversal region larger than the nozzle, which is commonly referred to as the virtual source.[6] This virtual source is restricted by a glass microskimmer of 1.2 ± 0.1 μm diameter for the helium microscopy measurements. For the D_2 focusing experiment a 46 μm glass skimmer was used. In this case the main aim was to demonstrate that a high intensity focus, fit for diffusion experiments, can be achieved. The skimmer size was therefore chosen to be larger than the virtual source at 10 bar D_2 to ensure a large detector count rate.

The nozzle was kept above room temperature; 320 K for helium and 305 K for D_2. The helium beam's average energy was 68 meV equating to a de Broglie wavelength λ of 0.055 nm. The nozzle temperature for the D_2 beam sets the average beam energy to 71.8 meV equivalent to a wavelength of 0.053 nm. Both were determined in time-of-flight (TOF) experiments. The spread in energy parallel to the beam, being a function of nozzle pressure and temperature, is commonly characterized using speed ratios, which were also determined using TOF. Speed ratio S is defined by $S^2 = mv^2/2kT$, where m is particle mass, v is particle speed, k is the Boltzmann constant, and T is the parallel temperature in the beam's frame of reference.[25] The speed ratio is related to the parallel speed distribution with average speed v and full width at half maximum (FWHM) Δv by $S = 2\sqrt{\ln(2)}(v/\Delta v) \simeq 2\sqrt{\ln(2)} \times (\lambda/\Delta\lambda)$. The nozzle pressures of $p_0 = 185$ bar and $p_0 = 170$ bar applied for generating the transmission micrographs result in speed ratios $S = 135 \pm 5$ and $S = 122 \pm 5$, respectively, for helium and $S = 24 \pm 1$ for D_2.

The beams were focused using a freestanding Fresnel zone plate produced using electron beam lithography by Rehbein[26] in the group of Günter Schmahl at the Institute for X-ray Physics in Göttingen. The scanning electron micrograph in Fig. 2 shows a detail of the zone plate employed for creating the presented images. The diameter of the zone plate is 540 μm with an outermost zone width of 50 nm. Also, the zeroth diffraction order is blocked by a central disk of about 162 μm in diameter. For the wavelength of the helium atoms noted above the zone plate has a focal length of about 506 mm. The source distance of $g = 1492 \pm 5$ mm resulted in an image distance of $b = 763 \pm 5$ mm, as expected, and setting the magnification to $M = b/g = 0.51 \pm 0.01$. The zone plate has inherent chromatic aberration as mentioned earlier, which is also the limiting factor for the smallest focus width in our experiment of less than 2 μm.

The imaged sample is shown in a scanning electron micrograph shown in Fig. 3(a). It is a carbon foil suspended on a quadratic copper grating. The carbon foil has holes of about 2 μm. The sample is mounted along with an order

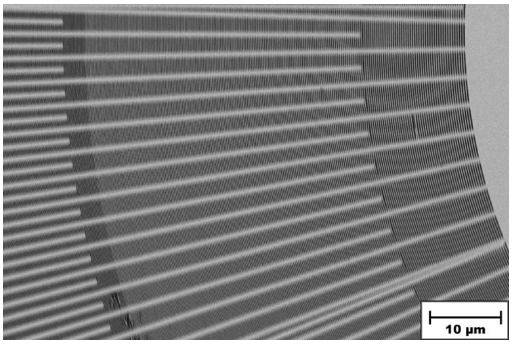

FIG. 2. Supersonic expansion helium and D_2 beams were focused using a freestanding Fresnel zone plate made of nickel on a silicon membrane using electron beam lithography. The scanning electron microscopy image shown in this figure is a close-up of the innermost zones of the zone plate. The broad horizontal lines are support bars and the central circular disk, which can be seen partially to the right of the image, is used to block the zeroth order for increased contrast. The zone plate has 2700 zones with an outermost zone width of about 50 nm. The concentric circular modulations visibly centered at the top of the image are artifacts (Moiré fringes).

selecting aperture of 100 μm diameter in order to suppress the zeroth diffraction order. A piezodriven holder with a maximal range in both directions normal to the beam of 80 μm is used to step the sample across the focus. A shadow image is recorded this way using an electron bombardment detector with magnetic mass selection and an off-the-shelf channeltron resulting in the above mentioned efficiency for the detection of helium of about 2×10^{-6}.

The D_2 beam focus was measured by replacing the carbon foil with a 5 μm by 3 mm slit and scanning the piezotable across the focused spot. The position of the focal plane along the optical axis was determined experimentally by moving

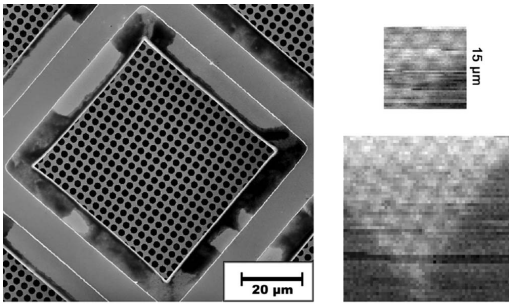

FIG. 3. Sample shown in the scanning electron micrograph (a) is a carbon holey foil on top of a copper mesh (Quantifoil®, R2/1). The holes have a diameter of about 2 μm. The two small images (b) are transmission helium microscopy scans of the same sample. The upper image is 15×15 μm^2 and took 14.6 h to record. The bottom one is 30×30 μm^2 and took 14 h to record. The nozzle pressures were $p_0 = 185$ bar and $p_0 = 170$ bar, respectively, resulting in beam focuses of less than 2.0 μm and about 2.3 μm, respectively. In the top micrograph the size of steps made between pixels was 0.3 and 0.5 μm for the other one.

this slit together with the detector closer and further away from the zone plate. A minimal focus was achieved at a sampling distance of $b=800\pm5$ mm. The focal length of the zone plate for the D_2 de Broglie wavelength is $f=520\pm1$ mm. The expected sampling distance corresponding to this focal length is $b=798\pm2$ mm, which is in good agreement with the experimental value noted above. The resulting magnification of the configuration was $M=0.54\pm0.01$. Finally, using D_2 has the further advantage of an approximately three times higher detector efficiency when compared to helium.[25]

Considerable efforts were put into keeping laboratory temperature fluctuation to a minimum (<0.2 K peak to peak) as well as apparatus vibration (<1 μm rms).

III. RESULTS

The new helium micrographs are shown in Fig. 3(b). The upper image is the highest resolution image created so far (step size of 0.3 μm and focus width of less than 2 μm). The depicted signal has an intensity of about 400 s^{-1} including a background of about 300 s^{-1}. The 2 μm holes are clearly resolved in spite of image defects caused by changes in signal background possibly due to outgassing (the sample was mounted only a few hours before we started recording the image). The recording times were about 15 h. This is still much to long for most practical usage. The long recording time is caused partly by the inefficiency of the detector and partly by the fact that it only records 1 pixel at a time. Keeping the vacuum apparatus stable both in temperature and position over such extended periods is very difficult. The distortion of the images is most likely due to small variations in the laboratory temperature distribution not picked up by the adapted air-conditioning system. The images demonstrate the presently best spatial resolution available with which a porous or permeable membrane can be illuminated.

A slit scan of the D_2 focus is shown in Fig. 4. It has a width of 16.0 ± 0.5 μm FWHM. This needs to be deconvoluted from the 5 μm slit function by taking the root of the subtracted squared widths, resulting in an actual focus width of 15.2 ± 0.5 μm FWHM. This value can be well accounted for by considering chromatic aberration of the zone plate. As can be deduced from the theory presented in Sec. IV, the chromatic point spread function (PSF) for a beam with speed ratio $S=24$ and an effective zone plate radius[8] $r_N=215$ μm has a width of 14.9 ± 0.6 μm. This confirms that the width of the virtual source is much smaller than the skimmer width, as expected. Note that the attained focus is much larger than in the helium experiments.

IV. THEORY

Here we discuss the limitations of Fresnel zone plate focusing. The transversal width w of the chromatic PSF is governed by the following relation:[27]

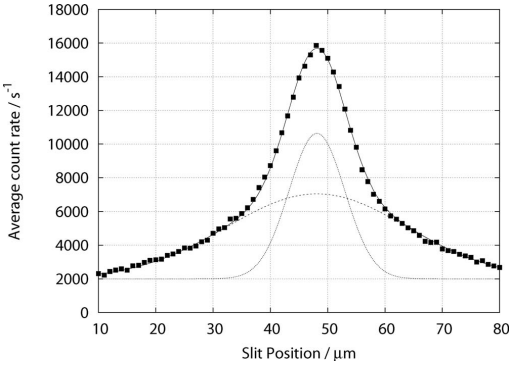

FIG. 4. This graph shows a slit scan of the first two-dimensional focus of a neutral molecular beam. The focus was recorded by stepping a 5 μm slit horizontally in the focal plane of the zone plate. The step size was 1 μm and the measuring time for each data point was 1 s. The nozzle pressure was 10 bar and its temperature was set to $T=305$ K. The continuous line shows a fit of the data by a double Gaussian convoluted with a 5 μm slit function. The two Gaussians are shown separately as dashed lines. The deconvoluted measured FWHM was 415.2 ± 0.5 μm.

$$w=\frac{r_N}{\lambda/\Delta\lambda}=2\sqrt{\ln(2)}\frac{r_N}{S}, \tag{1}$$

where r_N is the radius of the zone plate. This formula can be derived with the help of the drawing shown in Fig. 5. The focal length is proportional to $1/\lambda$. The minimal transversal focus width is indicated by w. One can deduce from the geometry that the following two equations must be satisfied: $(w/2)/(\Delta f-a)=r_N/f_m$ and $(w/2)/a=r_N/(f_m+\Delta f)$, with solutions $a=(f_m+\Delta f)/[2f_m/(\Delta f+1)]$ and $w=r_N/[f_m/(\Delta f+\frac{1}{2})]$. We further note that $f_m/\Delta f+1/2=\lambda/\Delta\lambda$ giving the above equation. Equation (1) is depicted in Fig. 6 for experimentally relevant values of the parameters S and r_N.

As it is clear now, the two approaches for reducing the size of the focal spot are either to provide a more monochromatic source with higher S or to use a zone plate with a

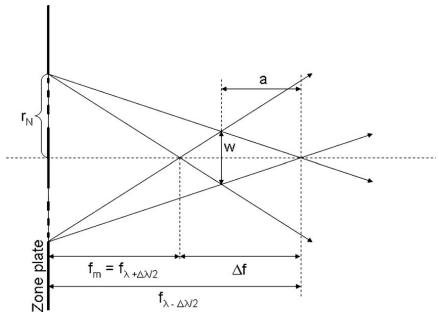

FIG. 5. This drawing depicts the effect of a zone plate's chromatic aberration on focus width w. The zone plate's radius is given by r_N and the difference between two focal lengths arising from two different wavelengths is labeled Δf.

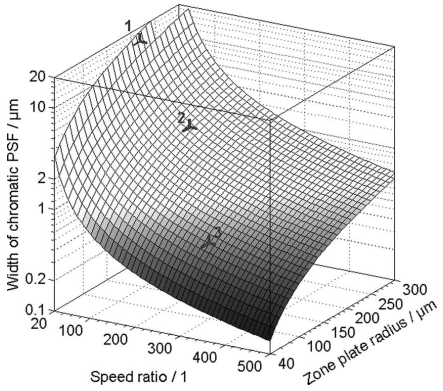

FIG. 6. Width of the chromatic PSF of a zone plate is shown as a function of speed ratio and zone plate radius. The dark shaded area indicates the region where chromatic broadening is less than one micrometer. Point 1 shows the location of the D_2 experiment within the graph. Point 2 indicates the configuration for the helium microscopy imaging, and point 3 locates the current limit of our apparatus of about 500 nm chromatic broadening.

smaller diameter (fewer zones). The first can be achieved to a certain extend by cooling the beam source nozzle or increasing source pressure. Both lead eventually to clusters forming in the beam, resulting in a reduction in the beam's speed ratio, and require higher source chamber pumping speeds. The present experiments for helium were carried out using speed ratios of 122 and 135. Using a beam cooled to 77 K (liquid nitrogen cooling) in theory it should be possible to achieve a speed ratio of about 500.[25] This would limit focal chromatic broadening to about 300 nm assuming that the zone plate is stopped down to a diameter of 200 μm. Even higher speed ratios $S>1000$ have been achieved using pulsed sources,[28] which requires large chamber dimensions, however. A speed ratio of 1000 would lead to a focus of 170 nm when using a 200 μm diameter zone plate. In order to achieve diffraction-limited focusing a speed ratio roughly larger than the number of zones of the zone plate is necessary.[29] Another method to achieve high speed ratios is velocity selection, but this also implies a significant loss in intensity.

On our apparatus maximal achievable speed ratios should be closer to 300, limited by pumping speeds, which should limit chromatic broadening to 500 nm (using a 200 μm diameter zone plate, see point 3 in Fig. 6). The use of smaller zone plates naturally also entails a counterproductive reduction in focal intensity and numerical aperture. We deduce that submicron resolution can be achieved even with the current setup, even at low signal-to-noise ratios and only in transmission mode. This assumes that chromatic broadening is the limiting factor. A configuration using a 1 μm skimmer with a magnification of 0.5 would allow focal widths of about 500 nm, which we hope to demonstrate soon.

An option for reducing longitudinal chromatic aberration is the move from first order to third order focusing (there is no second order focus for zone plates with open ratio 1:1).[27] However, this merely results in a smaller spreading of the various focal lengths along the optical axis, while transversal broadening remains the same, as can be seen from Eq. (1). Third order diffraction, while resulting in a reduction in focal intensity by a factor of $\frac{1}{10}$, would only improve diffraction-limited resolution.[30]

A more involved strategy for a reduction in focus size is the possibility of correcting chromatic aberration of zone plate optics within the beam's chromatic bandwidth. This has been of importance in the field of short wavelength electromagnetic radiation optics (extreme ultraviolet and x ray), where zone plates are equally vital tools. While highly chromatic sources are available there, they are not as compact as one would like. Therefore it has been suggested a number of times to combine zone plates with refractive optics to correct for chromatic aberration within the bandwidth of tabletop sources.[29,31] A similar approach for atom optics could lead to focusing in the 1 nm regime.

V. CONCLUSION

We have presented new neutral helium microscopy images with the hitherto best resolution of less than 2 μm. Furthermore, we have demonstrated the first focusing of neutral ground-state molecules using a Fresnel zone plate: A supersonic D_2 beam has been focused down to 15.2 ± 0.5 μm and we have argued that focused beams of molecules open new possibilities in the investigation of diffusion properties of materials. This is of particular interest, for example, for fuel cell membrane research and the study of hydrogen storage materials. We also showed calculations indicating that 300 nm is the best spot size which can be achieved with presently available techniques. To bring zone plate focusing of neutral atoms and molecules to its full potential (diffraction-limited focusing), advances in detector technology and methods tackling the problem of chromatic aberration need to be made. Field ionization detectors have the potential to solve the first of those issues. The combination of zone plates with refractive elements potentially is an option to reduce chromatic aberration. This could be achieved as well by velocity selection, yet at the cost of intensity. Alternatively mirror focusing, which is inherently achromatic is an option.

ACKNOWLEDGMENTS

The authors are indebted to Stefan Rehbein and Günter Schmahl for providing us with state-of-the-art zone plates. We thank Gianangelo Bracco for our nozzle design and numerous ideas and Egil S. Erichsen for assistance with the scanning electron micrograph in Fig. 2. This work was supported by the Bergen Research Foundation (the recruitment program) (http://www.uib.no/bfs/).

[1] M. Knoll and E. Ruska, Z. Phys. **78**, 318 (1932).
[2] G. Binnig, H. Rohrer, C. Gerber, and E. Weibel, Phys. Rev. Lett. **49**, 57 (1982).
[3] D. Farias and K.-H. Rieder, Rep. Prog. Phys. **61**, 1575 (1998).
[4] F. Hofmann and J. P. Toennies, Chem. Rev. (Washington, D.C.) **96**, 1307 (1996).

[5]L. Pedemonte and G. Bracco, J. Chem. Phys. **119**, 1433 (2003).
[6]T. Reisinger, G. Bracco, S. Rehbein, G. Schmahl, W. E. Ernst, and B. Holst, J. Phys. Chem. A **111**, 12620 (2007).
[7]B. Holst and W. Allison, Nature (London) **390**, 244 (1997).
[8]M. Koch, S. Rehbein, G. Schmahl, T. Reisinger, G. Bracco, W. E. Ernst, and B. Holst, J. Microsc. **229**, 1 (2008).
[9]B. Holst, Nature Research Highlights, Nature (London) **451**, 226 (2008).
[10]Carl Zeiss SMT AG, 2007, www.smt.zeiss.com
[11]L. Zhou, Renewable Sustainable Energy Rev. **9**, 395 (2005).
[12]L. de Broglie, Nature (London) **112**, 540 (1923).
[13]O. Carnal, M. Sigel, T. Sleator, H. Takuma, and J. Mlynek, Phys. Rev. Lett. **67**, 3231 (1991).
[14]R. B. Doak, R. E. Grisenti, S. Rehbein, G. Schmahl, J. P. Toennies, and C. Wöll, Phys. Rev. Lett. **83**, 4229 (1999).
[15]E. Hecht, *Optics*, 4th ed. (Addison-Wesley, Reading, MA, 2002).
[16]K. Fladischer (unpublished).
[17]B. Samelin, M.S. thesis, Georg-August-Universität zu Göttingen, 1993.
[18]F. S. Patton, D. P. Deponte, G. S. Elliott, and S. D. Kevan, Phys. Rev. Lett. **97**, 013202 (2006).
[19]R. B. Doak, Y. Ekinci, B. Holst, J. P. Toennies, T. Al-Kassab, and A. Heinrich, Rev. Sci. Instrum. **75**, 405 (2004).
[20]J. Piskur, L. Borg, A. Stupnik, M. Leisch, W. E. Ernst, and B. Holst, Appl. Surf. Sci. **254**, 4365 (2008).
[21]D. J. Riley, M. Mann, D. A. Maclaren, P. C. Dastoor, W. Allison, K. B. K. Teo, G. A. J. Amaratunga, and W. Milne, Nano Lett. **3**, 1455 (2003).
[22]D. A. MacLaren and W. Allison, Inst. Phys. Conf. Ser. **179**, 383 (2004).
[23]Y. Ekinci and J. P. Toennies, Phys. Rev. B **72**, 205430 (2005).
[24]R. Grisenti, W. Schöllkopf, J. Toennies, G. Hegerfeldt, and T. Köhler, Phys. Rev. Lett. **83**, 1755 (1999).
[25]*Atomic and Molecular Beam Methods*, edited by G. Scoles (Oxford University Press, Oxford, 1988).
[26]S. Rehbein, J. Phys. IV **104**, 207 (2003).
[27]A. G. Michette, *Optical Systems for Soft X-Rays* (Plenum, New York, 1986).
[28]J. Wang, V. A. Shamamian, B. R. Thomas, J. M. Wilkinson, J. Riley, C. F. Giese, and W. R. Gentry, Phys. Rev. Lett. **60**, 696 (1988).
[29]Y. Wang, W. Yun, and C. Jacobsen, Nature (London) **424**, 50 (2003).
[30]A. Takeuchi, Y. Suzuki, and H. Takano, J. Synchrotron Radiat. **9**, 115 (2002).
[31]G. K. Skinner, Appl. Opt. **43**, 4845 (2004).